JOURNAL OF PROPULSION AND POWER
Vol. 27, No. 2, March–April 2011

Characterization of Ion Cyclotron Resonance Acceleration for Electric Propulsion with Interferometry

Christopher Davis*
ElectroDynamic Applications, Inc., Ann Arbor, Michigan 48105
Brian Gilchrist†
University of Michigan, Ann Arbor, Michigan 48109
and
Jared Squire‡
Ad Astra Rocket Company, Webster, Texas 77598

DOI: 10.2514/1.48087

This paper describes the experimental characterization of single-pass ion cyclotron resonance heating as applied to acceleration of ions for electric propulsion. A millimeter-wave interferometer system has shown to be a clear and simple method of quantifying ion acceleration due to ion cyclotron resonance heating. The experimental work was done on the VX-10 experiment of the variable specific impulse magnetoplasma rocket concept. The perpendicular velocity of the ions generated by ion cyclotron resonance heating was converted into axial velocity by the decreasing gradient of the axial magnetic field at the exhaust of the propulsion system from conservation of the magnet moment. This increase in axial velocity is predicted to cause a decrease in density due to conservation of current in the plasma. Interferometer density measurements were taken at three different locations on the VX-10 experiment upstream and downstream of the ion acceleration zone. A clear measurement of a 25% density drop for helium and a 40% density drop for deuterium was measured downstream of the ion resonance zone characteristic of ion acceleration.

Nomenclature

B_{oz}	=	axial direct current magnetic field, T
$\boldsymbol{B}_{x,y,z}$	=	ion cyclotron resonance heating magnetic field vector components, T
c	=	speed of light
e	=	electron charge, C
$\boldsymbol{E}_{x,y,z}$	=	ion cyclotron resonance heating electric field vector components, V/m
f	=	frequency, Hz
f_p	=	plasma frequency, Hz
m_i	=	ion mass, kg
n	=	plasma density, m^{-3}
t	=	time, s
$\boldsymbol{V}_{x,y,z}$	=	ion velocity vector components, m/s
v_{gc}	=	guiding center velocity, m/s
ε_o	=	free-space dielectric constant
ω	=	radial frequency, rad/s
ω_{ci}	=	ion cyclotron frequency, rad/s

I. Introduction

ION cyclotron resonance heating (ICRH) is a relatively new experimental method [1] for accelerating propellant flow in electric propulsion systems. An ICRH system is actively being studied with special features allowing for variable specific impulse. This system is called the variable specific impulse magnetoplasma rocket (VASIMR) [2]. The experimental work presented in this paper on ICRH was done on a prototype of a proof of concept of the VASIMR engine, the VX-10 [3]. The diagram in Fig. 1 shows the basic layout of the VX-10 version of the VASIMR concept. The engine consists of three sections. The forward section is where the injection of the propellant gas and its ionization is using a helicon source. In this stage, a cold and dense plasma is produced by ionizing a gas (in most cases, helium or hydrogen) using a helicon ionization source. Helicons are propagating wave modes in a finite, axially magnetized plasma column [4]. The driving frequencies for helicon waves are typically 1–50 MHz, the direct current (DC) magnetic field is about 0.02–0.2 T, and the densities are on the order of 10^{11}–10^{14} cm^{-3}. Typical operating conditions for the VASIMR experiment are 0.18 T DC magnetic field, 20 MHz helicon frequency, and densities in the area of 10^{12} cm^{-3}. The middle section amplifies or heats the plasma using ICRH, and the aft cell converts the energy of the plasma into a directed flow using a magnetic nozzle. The focus of this paper is on the ICRH amplification section.

The experimental work presented in this paper on ICRH is part of the first work to experimentally verify this process.

Received 11 November 2009; revision received 15 November 2010; accepted for publication 17 November 2010.

*Senior Engineer, 3600 Green Court, Suite 300.
†Professor, Electrical Engineering and Computer Science; and Atmospheric, Oceanic, and Space Sciences, 1301 Beal Avenue.
‡Director of Research, 141 West Bay Area Boulevard.

II. Ion Cyclotron Resonance Heating Concept

The basic principle of ICRH is that a RF wave is launched into a magnetized plasma where it then accelerates the ions by increasing their rotational speed around the magnetic field lines [5]. Assuming the wave is traveling parallel to the magnetic field lines, the electric field vector of the left-hand component of the wave will rotate around the field lines with a frequency ω in the same direction as the ion's cyclotron motion about the field lines. Consequently, for $\omega \approx \omega_{ci}$, the force from the electric field of the wave on the ions will result in a continuous rotational energy gain. The perpendicular velocity of the ions generated by ICRH is then converted into axial velocity by the decreasing gradient of the axial magnetic field at the aft cell of the propulsion system from conservation of the magnet moment. This increase in axial velocity is predicted to cause a decrease in density due to conservation of particles in the plasma [6].

We consider collisionless plasma with cold ions in an equilibrium axisymmetric mirror magnetic field about the z axis (along the centerline of the VASIMR experiment). The model is based on the work presented in [7]. It is assumed that the axial DC magnetic field is much stronger than the radial field. The ICRH RF wave has a direction of propagation that is nearly parallel to the magnetic field lines. To find the ion velocity, the ion momentum balance equation is used. The following assumptions are made to simplify the equation:

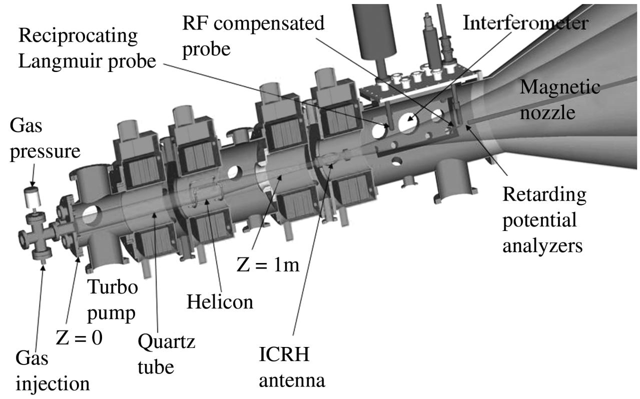

Fig. 1 Basic layout of the VX-10 VASIMR experiment.

1) The x and y derivatives of the RF electric and magnetic fields are small near the resonance.

2) $E_z = 0$ because of the high conductivity of the electrons.

3) V_z and n are time independent.

Using the preceding assumptions, the equation for perpendicular components of the ion velocity (V_x and V_y) can be found as shown next:

$$\frac{\partial V_x}{\partial t} + V_z \frac{\partial V_x}{\partial z} = \frac{eE_x}{m_i} + \omega_{\text{ci}} V_y \tag{1}$$

$$\frac{\partial V_y}{\partial t} + V_z \frac{\partial V_y}{\partial z} = \frac{eE_y}{m_i} + \omega_{\text{ci}} V_x \tag{2}$$

The spatial dependence of V_z (it is time independent) is determined by the momentum balance equation along z:

$$m_i V_z \frac{\partial V_z}{\partial z} = -\mu \frac{\partial B_{oz}}{\partial z} + q\langle V_x B_y - V_y B_x \rangle - m_i \frac{T_e}{m_i} \frac{1}{n} \frac{\partial n}{\partial z} \tag{3}$$

The three terms on the right-hand side of Eq. (3) represent the following, in order from left to right: 1) the force of the ion due to the gradient of the magnetic field, 2) the z component of the Lorentz force equation from the RF wave (RF pressure), and 3) the force associated with the ambipolar electric field.

The brackets in Eq. (3) represent an averaging of the RF pressure force over several ion gyrations, and $\mu = [m_i(V_x^2 + V_y^2)]/2B_{oz}$, which is the ion magnetic moment.

Assuming the polarization of the incoming wave is circular, the electric field, as well as the x and y components of the magnetic field and ion velocity, have the following form [8]:

$$A_+ = \frac{A_x + jA_y}{\sqrt{B_{oz}/B_*}} e^{i\omega t} \tag{4}$$

where A_+ is either V_+, B_+, or E_+. B_* is the value of the DC magnetic field at resonance. The factor $\sqrt{B_{oz}/B_*}$ represents the fact that the perpendicular components will decrease as the magnetic field drops off. Therefore, to get physical quantities out of the preceding equations, $\sqrt{B_{oz}/B_*}$ has to be multiplied to any perpendicular components (A_+) after solving for them.

Using all of the preceding equations and assumptions, the following set of equations for E_+, B_+, V_+, V_z, and n can be defined. E_+, B_+, and V_+ in the following equations are the complex amplitudes of the RF electric and magnetic fields and the perpendicular velocity. The velocity V_+ represents the rotational velocity of the ions:

$$V_z \frac{\partial V_z}{\partial z} = -\frac{c^2 \varepsilon_o}{2m_i n} \frac{B_{oz}}{B_*} \frac{\partial |B_+|^2}{\partial z} - \frac{|V_+|^2}{2B_*} \frac{\partial B_{oz}}{\partial z} - \frac{c_s^2}{n} \frac{\partial n}{\partial z} \tag{5}$$

$$V_z \frac{\partial V_+}{\partial z} = \frac{e}{m_i} E_+ + j(\omega - \omega_{\text{ci}}) V_+ \tag{6}$$

$$\frac{B_*}{B_{oz}} n V_z \equiv j = \text{constant} \tag{7}$$

Equation (5) is the axial momentum balance equation for the ions, and Eq. (6) is the perpendicular momentum balance equation. Equation (7) is the continuity of current within the plasma. The first term on the right-hand side of Eq. (5) can be approximated as zero, due to the resonance area being much shorter than the RF wavelength of the ICRH wavelength, causing the ICRH electric and magnetic fields to change very little in the resonance zone.

III. Experimental Setup

To characterize this density decrease during ion cyclotron heating, a single-channel interferometer system was developed and implemented on the VX-10, an experimental version of the VASIMR. Millimeter-wave interferometry is inherently nonintrusive and avoids the problems of probe heating and local plasma perturbations of in situ techniques in dense energetic plasmas [9,10]. The experimental setup is described next.

Figure 2 shows a diagram of the primary interferometer system used for this research to measure the density change predicted to occur during ICRH acceleration, as discussed previously. The plasma is represented in the figure and is flowing out of the page. The basic operation of the system is as follows. The oscillator generates 15 dBm of power at 70 GHz. The signal is then split by a 3 dB coupler, sending part of the signal to the antennas to be transmitted through the plasma and the other part to the local oscillator power for the mixer. The antennas used are 25 dB standard gain horns. The face of the horn is 3.85 cm (1.51 in.) by 3.10 cm (1.2 in.), and the antenna has a length of 8.13 cm (3.2 in.). The 3 dB beam width of the horn is approximately 10 deg. The isolators attenuate the signal traveling in the reverse direction by 20 dB. The isolators were put in to protect the oscillator from power reflections and to reduce internal reflections that could interfere with phase accuracy. It was also necessary to magnetically shield the isolators from the high ambient magnetic field.

Since the mixer is mixing two signals that are of the same frequency, the intermediate frequency output of the mixer has the following form, shown in Eq. (4):

$$V(t) = A \sin[\phi_o(t) + \theta_o] + V_{\text{off}} \tag{8}$$

where ϕ_o is the phase shift through the plasma path, which varies as a function of time, θ_o is the phase offset, and can be adjusted using the phase shifter, V_{off} is the DC voltage offset of the mixers from zero, and A is the amplitude of the voltage swing of the mixers. Using the phase shifter shown on the system diagram, θ_o is adjusted so that $V(t)$ is approximately equal to V_{off} with no plasma present. Then, taking the difference between the plasma $[A \sin(\phi_p + \theta_e) + V_{\text{off}}]$ and no plasma voltage $[A \sin(\theta_e) + V_{\text{off}}]$ gives the following expression:

$$\Delta V(t) = A\{\sin[\phi_p(t) + \theta_e] + V_{\text{off}} - \sin(\theta_e) - V_{\text{off}}\} \tag{9}$$

where θ_e is the error in calibrating $V(t)$ to be equal to V_{off} without the plasma present or, in other words, the voltage output of the mixer

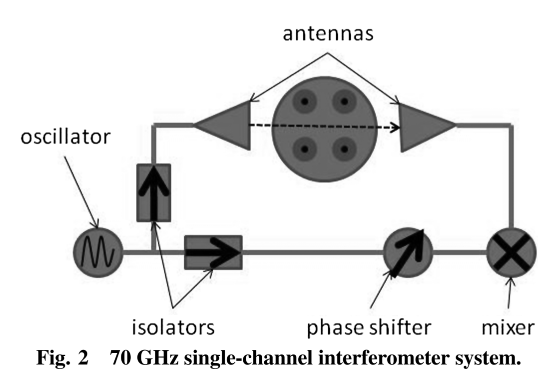

Fig. 2 70 GHz single-channel interferometer system.

with no plasma is equal to DC voltage offset V_{off} of the mixer. It is assumed this offset voltage is a characteristic of the mixer and does not change with the plasma present. Ideally, θ_e is equal to zero, and $\phi_p(t)$ is the net phase shift through the plasma. If the assumption is made that θ_e is small enough to have a negligible effect, then the net phase shift through the plasma can be simplified to Eq. (6):

$$\phi_p(t) = \sin^{-1}\left(\frac{\Delta V(t)}{A}\right) \tag{10}$$

The accuracy of setting $V(t)$ equal to V_{off} with no plasma present was estimated to be no worse than 10 mV. The output voltage of the interferometer with no plasma present can also drift over time. By recalibrating the interferometer periodically, it was found that the maximum drift of $V(t)$ from V_{off} was no worse than 20 mV. The amplitude of the voltage swing A varied from 450 to 800 mV, depending on the experimental setup, specifically the distance between the antennas. Assuming the worst case scenario that $A = 450$ mV, then the maximum value of $\theta_e = \sin^{-1}(\pm 30/450) \approx \pm 4°$, which would cause a measured phase error of about $\pm 4\%$ at a measured phase shift of 40 deg (i.e., $40 \pm 1.6°$). which was the maximum phase shift measured with the single-channel interferometer system. Other sources of error include temperature drift of the oscillator, approximated at $\pm 2.5\%$, and reflections, approximated at $\pm 3\%$ [11].

The peak plasma density can then be calculated from the phase shift using the following relation, which is valid if the interferometer frequency is greater than three times the plasma frequency [10]:

$$n_o = \left(\frac{4\pi\varepsilon_o m_e c f}{e^2}\right)\Delta\theta \frac{1}{\int_{-\infty}^{\infty} e^{-r^2/\sigma^2}\,\mathrm{d}r} \tag{11}$$

$$\int_{-\infty}^{\infty} e^{-r^2/\sigma^2}\,\mathrm{d}r$$

in Eq. (11) represents the integral of the normalized density profile, which was determined through Langmuir probe measurements on the VX-10 experiment [11].

IV. Measurement Results

To characterize this predicted density drop during ion cyclotron heating, interferometer measurements were taken at three different locations on the VX-10 experiment. Figure 3 shows the positions of the three measurement ports. Figure 4 shows a diagram of the calculated axial magnetic field profile with the location of the measurement ports and ICRH antenna.

As is illustrated in Fig. 4, port 3 is located before the ICRH antenna and is upstream of the resonance point. Port 1 and port 2 are located well downstream of the ICRH resonance point. Experiments were run with both helium and deuterium gas. Table 1 summarizes the experiment parameters for the helium and deuterium tests presented.

A. Measured Helium Density Drop

Figures 5 and 6 show measurement results illustrating a clear density drop with the application of ICRH power. The data were taken for a helium discharge. The measurements were taken with a helicon source power of 3.5 kW, an ICRH power of 1.5 kW, and a gas flow rate of 110 standard cm^3/ min (sccm). The ICRH frequency was set to 1.85 MHz, which corresponds to a resonance point at 0.48 T. The helicon power turned on at approximately 0.36 s and turned off at 2.3 s, as is illustrated in Figs. 5–7. ICRH power was only applied for a fraction of the total pulse, 200 ms, to illustrate the net density drop. There is a clear density reduction of approximately 25% at port 1 and port 2 when ICRH power is applied as expected.

The neutral pressure at the ports increases approximately linearly from 0.5×10^{-4} to 1.5×10^{-4} Torr during the length of the pulse. The increase in density over the duration of the pulse at ports 1 and 2 is believed to be due to this increasing neutral pressure, causing an increase in charge exchange collisions that creates a slow-moving

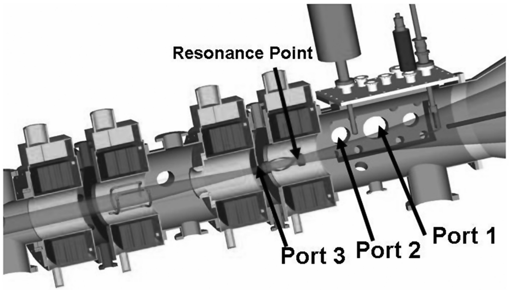

Fig. 3 Interferometer measurement locations on the VX-10 experiment.

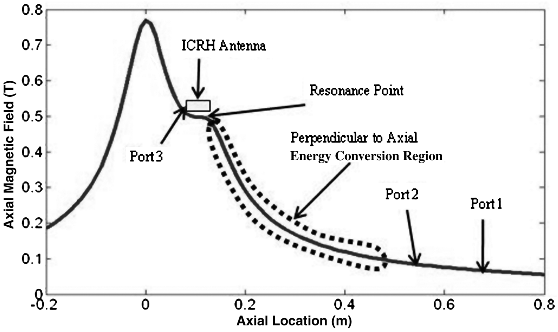

Fig. 4 Axial magnetic field profile for helium on the VX-10 experiment.

plasma component and, by conservation of current, increases the density [11]. The increase in neutral pressure is caused by the vacuum chamber pumping not being able to keep up the gas flow into the chamber.

Figure 7 shows density measurements taken at port 3 of the VX-10 experiment. Again, ICRH power was only applied for a fraction of the total plasma shot with an ICRH power set to 1.5 kW.

The increase in density at port 3 is most likely caused by additional ionization of the background neutral density due to the ICRH power being coupled to plasma, not at the resonance frequency. An experiment was run using argon instead of helium gas but using an ICRH frequency magnetic field profile in the helium range (1.85 MHz) so that the resonance point was outside the axial field values of the experiment. Figure 8 shows density measurements taken at port 1.

As shown in Fig. 8, the density increases, as opposed to decreases, downstream of the resonance, indicating that the plasma is no longer being accelerated and the ICRH energy is simply ionizing additional neutrals similar to what may be occurring at port 3 with the helium plasma.

Figure 9 shows the calculated axial ion velocity versus axial distance along the VX-10, with the measurement ports and resonance point indicated on the plot using Eqs. (5–7) and measured parameters from the VX-10 experiment. The ICRH electric field was estimated based on the magnitude of the measured density drop. As has been discussed previously (see Sec. II), from conservation of current through the plasma ($nV_z =$ constant), the increase in axial velocity with cyclotron heating will be proportional to the decrease in density.

Figure 9 illustrates that, at port 3, the axial ion velocity is not changing, so a decrease in density should not be measured. While at ports 1 and 2, there is calculated to be a significant increase in the ion's axial velocity due to the perpendicular velocity gained by the ions as they passed through the resonance being converted to axial velocity by the magnetic field gradient. Therefore, the density at these ports should decrease, and the density decrease should be similar for both ports. This is consistent to what was measured in Figs. 6–8.

B. Deuterium Density Drop

Figure 10 shows three plasma shots superimposed, taken with deuterium at port 2 of the VX-10 experiment with an ICRH power

Table 1 Experimental parameters

Gas	Helicon power, kW	ICRH frequency, MHz	ICRH power, kW	Resonance field strength, T	Nominal flow rate, sccm	Electron temperature, eV
Helium	3.5	1.85	1.5	0.48	110	~8
Deuterium	9.0	1.85	1.5	0.24	70	~6

level of 1.5 kW applied for 500 ms, starting at 600 ms in the figure. The helicon source power was set at 9 kW. The flow rate for deuterium was 70 sccm. The helicon power and flow rate were changed to keep the plasma density similar to the helium experiments. The electron temperature of the plasma was measured to be around 6 eV for these experiments, and the pressure increase was the same as the helium case discussed previously.

The frequency of operation for the ICRH power source in the VX-10 experiment was kept the same as helium at 1.85 MHz; therefore, in order to set the ion cyclotron resonance point for deuterium at approximately the same location as helium, it was necessary to reduce the magnitude of the magnetic field. Since the ion cyclotron frequency is inversely proportion to the ion mass, reducing the field by a factor of two keeps the resonance location constant for deuterium and helium.

The average density reduction for deuterium was found to be 38%. The larger density reduction for deuterium can be attributed to better plasma loading at the ICRH antenna due to a denser plasma from the increased helicon power, less charge exchange collisions with helium [12,13], and the fact that the D2 ions are lighter then He ions, causing a higher velocity gain with the same ICRH power.

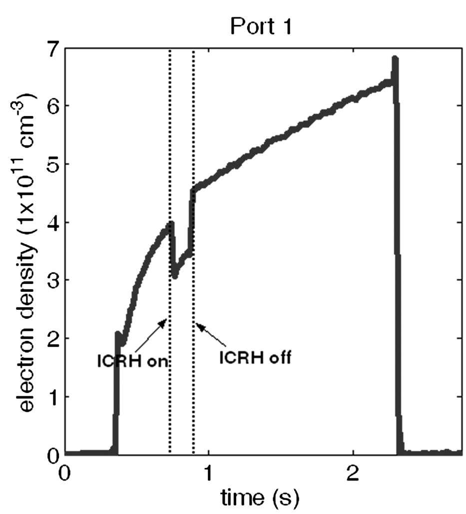

Fig. 5 Interferometer density measurements taken at port 1 of the VX-10 with ICRH applied for a fraction of the plasma shot.

C. Ion Cyclotron Resonance Heating Pulse Timing

Figures 11 and 12 show a scan in time of the ICRH power pulse at port 2 of the VX-10. Helium gas was used with 3.5 kW of helicon power and 1.5 kW of ICRH power at a gas flow rate of 110 sccm (see Table 1). The ICRH power pulse was started at varying times, as is shown in the plot in Fig. 11, and had a duration of 200 ms. The density ratio used here is defined as shown in Eq. (12):

$$n_r = \frac{n_o}{n_{\mathrm{ICRH}}} \tag{12}$$

where n_{ICRH} is the density measured after ICRH is turned on, and n_o is the density measured right before ICRH is turned on. The density value was averaged for 20 ms to determine n_o and n_{ICRH}.

As can be seen from Fig. 12, the density ratio is fairly independent of ICRH timing within the shot. The error in the density drop measurements is estimated to be around 15% [11]. As mentioned previously, charge exchange collisions will increase throughout the length of the plasma pulse downstream in the VX-10 due to increasing neutral density. The charge exchange collisions in the plasma will cause an axially slow-moving component of the ion distribution that loses the energy acquired from ICRH as the ions move downstream. The average velocity, though, of the ion flow, with and without ICRH, would be slowed down by the same amount, which would give the same relative density drop throughout the length of the pulse, despite an increase in collisions slowing down the flow overall.

D. Gas Flow Rate

Figure 13 shows helium plasma with the experimental parameters in Table 1, except the flow rate is varied from 110, 80, and 50 sccm, as is shown in the figure at port 2 of the VX-10.

As can be seen from the figure, the density ratio also does not change as the gas flow rate is varied. The final velocity of the ions after passing through the resonance zone should only depend on the velocity that the ions enter the resonance zone, the ICRH electric field

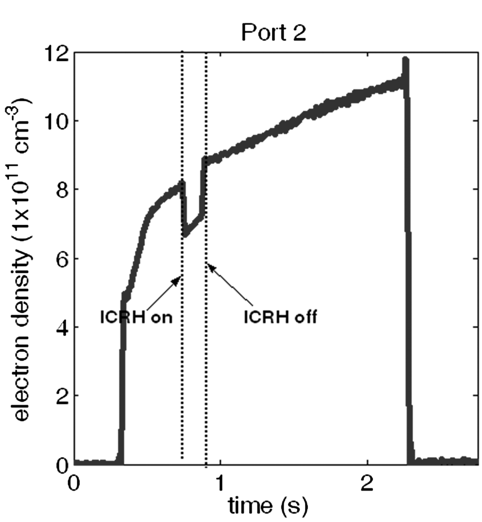

Fig. 6 Interferometer density measurements taken at port 2 of the VX-10 with ICRH applied for a fraction of the plasma shot.

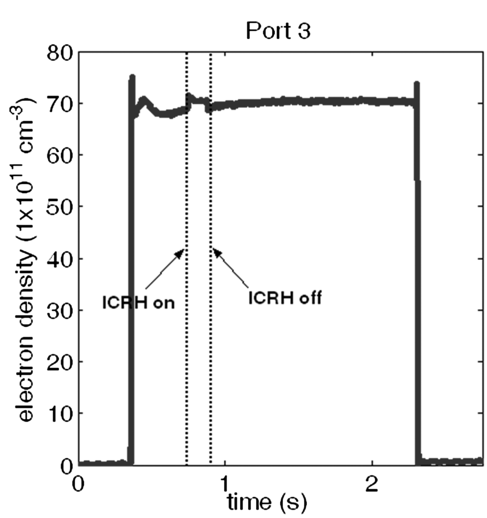

Fig. 7 Interferometer density measurements taken at port 3 of the VX-10 with ICRH applied for a fraction of the plasma shot.

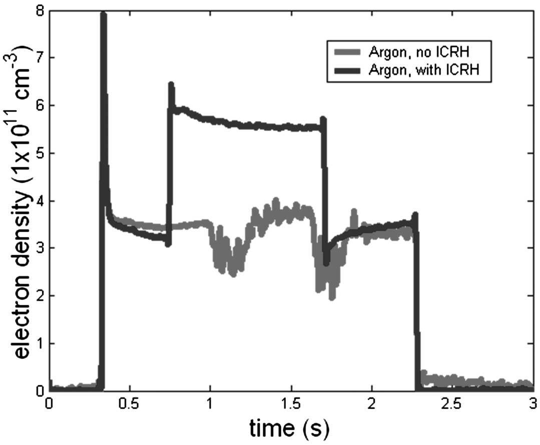

Fig. 8 Density measurements taken at port 1 of the VX-10 experiment with argon gas, with and without ICRH power.

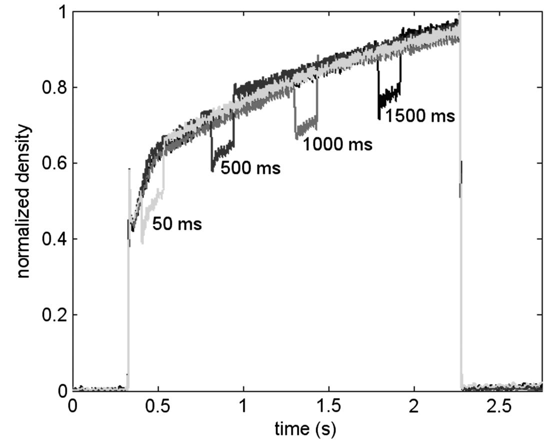

Fig. 11 ICRH pulse time scan for helium with 3.5 kW helicon power and 1.5 kW ICRH power.

for a given axial magnetic field profile, and the amount of perpendicular velocity gained by the ions from ICRH that has been converted to axial velocity, which will be constant at a given measurement port location.

The density ratio staying constant suggests that the ICRH electric field and the initial velocity of the ions into the resonance zone are remaining constant as the gas flow is being varied. This can be seen by Eq. (12), shown next [5]:

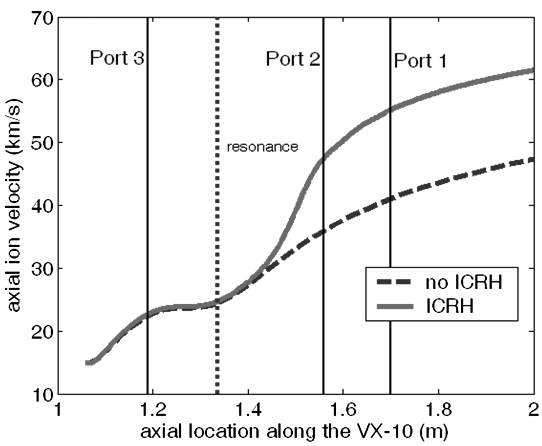

Fig. 9 Calculated axial ion velocity profile for helium with initial axial ion velocity of 15 km/s, Mach number M of 1.1, and $B_{\mathrm{res}} = 0.48$ T, and the magnetic field profile for helium in the VX-10.

$$(\Delta v) = \left(\frac{eE_+}{m}\right)\Delta t_{\mathrm{res}} \tag{13}$$

where E_+ is the ICRH electric field, Δt_{res} is the amount of time the ions are in the resonance zone, and Δv is the increase in ion perpendicular velocity. As can be seen from the equation, if the velocity of the ions entering the resonance increases, then Δt_{res} decreases, and the perpendicular velocity the ions gain (and hence, axial velocity downstream) decreases, and vice versa if the ion

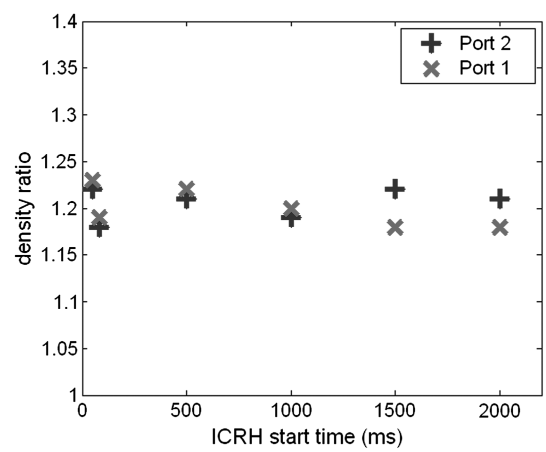

Fig. 12 Density ratio versus ICRH pulse timing at port 1 and port 2.

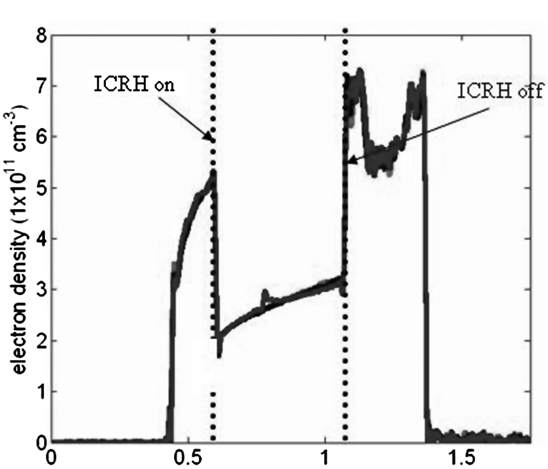

Fig. 10 Three density profiles for D_2 showing a typical density drop during ICRH measured at port 2 of the VX-10.

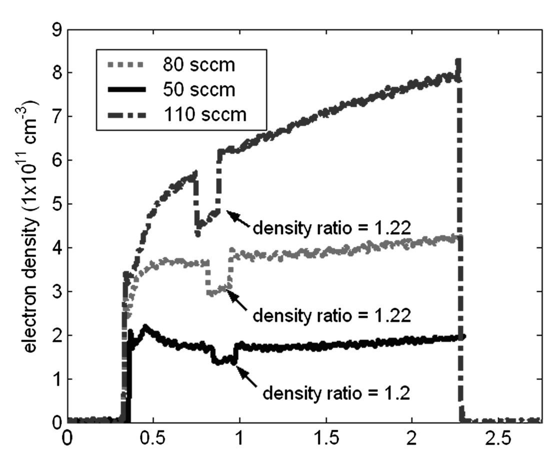

Fig. 13 Measured density ratio at port 2 of the VX-10 at gas flow rates of 50, 80, and 110 sccm.

velocity decreases. Additionally, if the ICRH electric field E_+ increases or decreases, Δv will increase or decrease.

V. Conclusions

The use of ion cyclotron resonance to heat ions is an emerging approach for space electric propulsion. The results presented in this paper were intended to contribute to the initial validation of this approach. This work was part of the first stage of an effort to experimentally validate the use of ICRH for application to electric propulsion devices.

The density drop due to ICRH acceleration was characterized by taking interferometer measurements at three locations along the VX-10. Measurements were made of the density drop in both helium and deuterium plasma discharges during ICRH under a variety of operating conditions, including gas flow rate and ICRH power pulse timing. A density drop was measured downstream of the ion resonance zone, characteristic of ion acceleration, and little change in density was measured upstream of the resonance zone where no acceleration was expected.

The interferometer system implemented on the VX-10 experiment during the course of this investigation provides a clear and simple method of quantifying ion acceleration due to ICRH. As experimental parameters are changed, interferometer measurements downstream of the energy conversion region can give a reliable measurement of how ion acceleration is affected.

References

[1] Chang-Diaz, F. R., "Rapid Mars Transit with Exhaust-Modulated Plasma Propulsion," NASA TP 3539, 1995.

[2] Chang-Diaz, F. R., "The VASIMR Rocket," *Scientific American*, Vol. 283, No. 5, Nov. 2000, pp. 91–97.

[3] Chang-Diaz, F. R., "The VASIMR Engine: Concept Development, Recent Accomplishments and Future Plans," *Fusion Science and Technology*, Vol. 43, 2003, pp. 3–9.

[4] Chen, F. F., and Boswell, R. W., "Helicons: The Past Decade," *IEEE Transactions on Plasma Science*, Vol. 25, No. 6, Dec. 1997, pp. 1245–1257.
doi:10.1109/27.650899

[5] Lieberman, M. A., and Lichtenberg, A. J., *Principles in Plasma Discharges and Materials Processing*, Wiley, New York, 1994, pp. 1245–1257.

[6] Arefiev, A., and Breizman, B., "Theoretical components of the VASIMR plasma propulsion concept," *Physics of Plasmas*, Vol. 11, No. 5, May 2004, pp. 2942–2949.
doi:10.1063/1.1666328

[7] Breizman, B., and Arefiev, A., "Single-Pass Ion Cyclotron Resonance Absorption." *Physics of Plasmas*, Vol. 8, No. 3, 2001, pp. 907–915.
doi:10.1063/1.1348034

[8] Arefiev, A., and Breizman, B., "Theoretical Components of the VASIMR Plasma Propulsion Concept," *Physics of Plasmas*, Vol. 11, No. 5, May 2004, pp. 2942–2949.
doi:10.1063/1.1666328

[9] Heald, C. B., and Wharton, M. A., *Plasma Diagnostics with Microwaves*, Wiley, New York, 1965.

[10] Hutchinson, I. H., *Principles of Plasma Diagnostics*, Cambridge Univ. Press, New York, 1987, pp. 103–154.

[11] Davis, C. N., "Experimental Validation of Single Pass Ion Cyclotron Resonance Absorption in a High Speed Flowing Plasma Applied to the Variable Specific Impulse Magnetoplasma Rocket (VASIMR)," Ph.D. Dissertation, Univ. of Michigan, Ann Arbor, MI, March 2006.

[12] McDaniel, E. W., *Collision Phenomena in Ionized Gases*, Wiley, New York, 1964.

[13] Chavers, G., "Recombination Processes in a Flowing Magnetized Plasma: Application to Ionization-Energy Recovery in the Variable Specific Impulse Magnetoplasma Rocket (VASIMR)," Ph.D. Dissertation, Univ. of Alabama, Tuscaloosa, AL, 2003.

J. Blandino
Associate Editor